ISSN 1808-8546 (ONLINE) 1808-3765 (CD-ROM)

ESTIMATIVA DO ÍNDICE DE ÁREA FOLIAR E DA FRAÇÃO DE COBERTURA DO SOLO NAS CULTURAS DE MILHO E SOJA USANDO NDVI[1]

LEORNAROD CHECHI[2]; MIRTA TERESINHA PETRY[3]; ZANANDRA BOFF DE OLIVEIRA[4]; MAX KLEBER LAURENTINO DANTAS[5]; CLARISSA MORAES DA SILVA[6] E ANDRESSA FUZER GONÇALVES[7]

[1] Parte do trabalho de dissertação de Mestrado do primeiro autor - Programa de Pós-Graduação em Engenharia Agrícola – UFSM

[2] Eng. Agrônomo, Mestre em Engenharia Agrícola, Programa de Pós-Graduação em Engenharia Agrícola, UFSM, Avenida Roraima, nº1000, Bairro Camobi, Santa Maria, RS, Brasil, CEP: 97195-000, leonardo.chechi@gmail.com

[3] Eng. Agrônoma, Doutora, Professora do Departamento de Engenharia Rural, UFSM, Avenida Roraima, nº1000, Bairro Camobi, Santa Maria, RS, Brasil, CEP: 97195-000, mirta.petry@gmail.com

[4] Eng. Agrícola, Doutora, Coordenadoria acadêmica Curso de Engenharia Agrícola, Campus da UFSM de Cachoeira do Sul. Rod. Taufik Germano, n.3013, Bairro Passo D'Areia, Cachoeira do Sul, RS, Brasil, CEP: 96503-205, zanandraboff@gmail.com.

[5] Eng. Agrônomo, Doutor em Ciência do Solo, UFSM, Avenida Roraima, nº1000, Bairro Camobi, Santa Maria, RS, Brasil, CEP: 97195-000, maxdantas22@gmail.com.

[6] Eng. Agrícola, Aluna de Mestrado do Programa de Pós-Graduação em Engenharia Agrícola, UFSM, Avenida Roraima, nº1000, Bairro Camobi, Santa Maria, RS, Brasil, CEP: 97195-000, clarissamoraes37@outlook.com.

[7] Acadêmica Curso de Agronomia, UFSM, Avenida Roraima, nº1000, Bairro Camobi, Santa Maria, RS, Brasil, CEP: 97195-000, dessa.fuzer@gmail.com.

1 RESUMO

Técnicas de sensoriamento remoto são utilizadas para avaliar mudanças na paisagem, como a fenologia, índice de área foliar (IAF), altura de plantas e fração de cobertura do solo (f_c). Os índices de vegetação (VI) têm sido relacionados às características biofísicas das culturas, como o IAF e a f_c. Assim, o NDVI (*Normalized Difference Vegetation Index*) tem sido utilizado para verificar a dinâmica da vegetação durante o ciclo de cultivo. Nesse estudo, o NDVI foi usado para estimar a f_c e o IAF das culturas soja e milho, visando monitorar o estado atual da vegetação para avaliações das necessidades hídricas das culturas. Observações à campo do IAF e f_c foram realizadas em intervalos de aproximadamente 8 dias. O NDVI foi derivado de imagens do satélite Sentinel (sensores 2A e 2B) e processado na biblioteca *open-source* do *Google Earth Engine*. Observou-se elevado ajuste entre os valores observados e simulados, com valores de b_0 próximos a 1,00, $R^2 > 0,99$ e RMSE variando de 0,02 a 0,05 para a f_c e de 0,29 a 0,61 para o IAF, indicando que os modelos propostos foram eficientes no monitoramento dessas variáveis biofísicas.

Palavras-chave: Sentinel, Google Engine, índices de vegetação, IAF.

CHECHI, L., PETRY, M.T., OLIVEIRA, Z. B., DANTAS, M. K. L., SILVA, C. M.; GONÇALVES, A. F.
ESTIMATION OF LEAF AREA INDEX AND FRACTON OF GROUND COVER OF CORN AND SOYBEAN CROPS USING NDVI

Recebido em 25/01/2021 e aprovado para publicação em 03/11/2021
DOI: http://dx.doi.org/10.15809/irriga.2021v26n3p620-637

2 ABSTRACT

Remote sensing techniques are used to assess changes in the landscape, such as phenology, leaf area index (LAI), plant height, and the fraction of ground cover (f_c). Vegetation indices (VI) have been related to biophysical characteristics of crops, such as LAI and f_c. Thus, the NDVI (Normalized Difference Vegetation Index) has been used to monitor vegetation dynamics throughout the crop development cycle. In this study, the NDVI was used to estimate the f_c and LAI of soybeans and corn crops, aiming to monitor the actual condition of the vegetation for crop water requirement assessments. Field observations of the LAI and f_c were carried out at intervals of approximately eight days. The NDVI used to estimate the f_c and LAI were derived from images of the Sentinel satellite (sensors 2A and 2B) and processed in the open-source Google Earth Engine library. A excellent fit between the observed and simulated values was observed, with values of b_0 close to 1.00, $R^2 > 0.99$, and RMSE ranging from 0.02 to 0.05 for fc and from 0.29 to 0.61 for LAI, indicating that the proposed models were efficient in the monitoring of these biophysical variables.

Keywords: Sentinel, Google Engine, vegetation indices, LAI.

3 INTRODUCTION

Crop biophysical characteristics vary spatially and temporally with vegetation growth, making them important for assessing crop phenological stages and scheduling management practices such as fertilizer application and irrigation management. Remote sensing (RS), through vegetation indices such as the normalized difference vegetation index (NDVI), offers several indicators of crop growth characteristics, such as the leaf area index (LAI) (YAO *et al*., 2015), the fraction of soil covered by the canopy (f_c) (ASADI *et al*., 2019), and biomass accumulation (GAO *et al*., 2018), which are important parameters for estimating biomass/grain production at the regional or farm level. The use of the NDVI to obtain canopy biophysical variables is possible because this index uses surface reflectance values obtained in the red and near-infrared ranges, which are a function of the chlorophyll content present in the leaves (LÓPEZ-URREA *et al*., 2020) and the structure and development stage of the canopy (PÔÇAS *et al*., 2020).

The f_c and LAI are associated with vegetation dynamics and are useful for mapping phenological stages, providing information on management practices and assessing productivity (SAKAMOTO *et al*., 2010). For crops such as soybean and corn, biophysical parameters describe their growth and development (DE LA CASA *et al*., 2018). Knowledge of the increase in LAI and the evolution of f_c in the different phases of the cycle allows the partitioning of crop evapotranspiration into plant transpiration and soil water evaporation (PAREDES *et al*., 2017; 2018), the determination of crop coefficients (ALLEN; PEREIRA, 2009), the estimation of the fraction of photosynthetically active solar radiation intercepted by the plant canopy (PURCELL *et al*., 2002), and the estimation of crop dry matter (LI *et al*., 2010). Consequently, f_c and IAF are commonly used as mandatory variables in agricultural models such as AquaCrop (FOSTER *et al*., 2017), SIMDualKc (PAREDES *et al*., 2017; 2018), and CSM-CROPGRO (RICHETTI *et al*., 2019), among others.

fc represents the vertical and horizontal density of vegetation, ranging from 0% (bare or no vegetation soils) to 100% when the canopy is complete or completely shades the soil (RITCHIE *et al*.,

2010). It is an excellent variable for estimating the LAI and biomass, which are parameters used in yield prediction models (BARKER *et al.*, 2018). Owing to the heterogeneity of vegetation at the regional scale, obtaining these parameters at the surface level is difficult, restricting or making it impossible to use process-based models (YAO *et al*., 2015). Therefore, a possible alternative, aiming to feed models and reproduce the current crop situation, is to associate the SR to extract biophysical parameters of vegetation, such as f_c and LAI (CAMPOS *et al*., 2018). The use of vegetation indices derived from SRs has become a very important tool for the calibration and validation of agricultural models (RICHETTI *et al*., 2019; CAMPOS *et al*., 2017; POÇAS *et al*., 2015; NEALE *et al*., 2012) because of the relationships between vegetation indices (IVs) and crop morphophysiological characteristics (LAI, f_c, and green plant matter) and other physiological processes that depend on radiation absorption by the canopy, including crop evapotranspiration (ET_c) (POÇAS *et al*., 2020; NEALE *et al*., 2012).

The timing of a specific phenological stage of crops such as soybean and corn can vary across locations and years due to factors such as the planting season, soil moisture, air temperature, and management practices (SAKAMOTO *et al., 2010). Therefore,* in situ observations of occurrence dates and values of these variables limit the use of many models, as observations require time and resources. Consequently, the results obtained through continuous surface observations of the LAI, plant height, and f_c are suitable for integration across spatial and temporal scales of interest over larger areas. Thus, the main objective of this study was to estimate the f_c and LAI of soybean and corn under irrigated and rainfed conditions via the NDVI.

4 MATERIALS AND METHODS

4.1 Site characterization and plant observations

The study consisted of field experiments carried out in a central pivot irrigated area (44 ha) and a rainfed area (3 ha) in the 2018/19 agricultural year in the Central Depression of Rio Grande do Sul (Figure 1). Both areas had similar soil and relief characteristics and were cultivated with the same corn hybrids and soybean cultivars.

Figure 1. Locations of the areas used in the study.

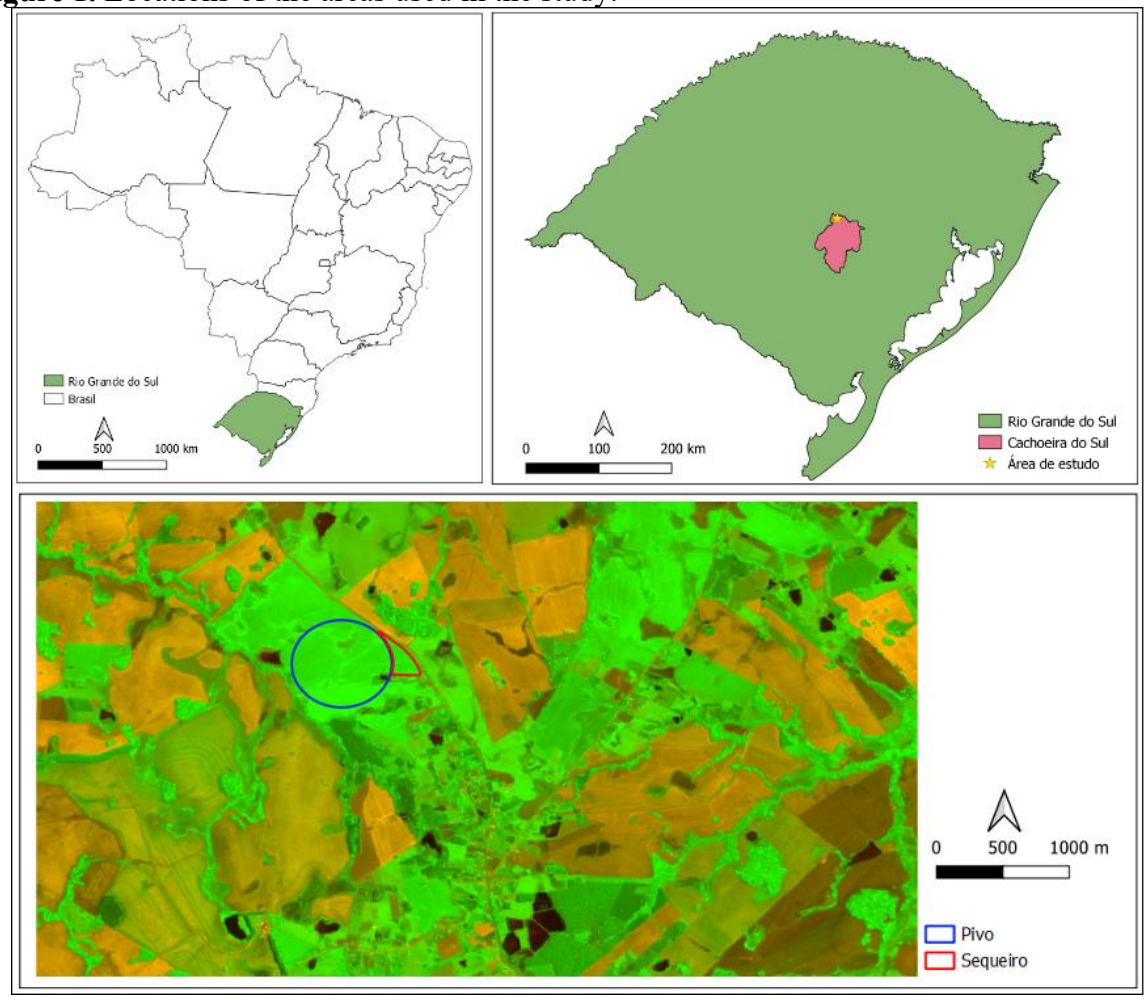

Source: Brazilian Institute of Geography and Statistics (IBGE) (2020) and Sentinel 2–November 2018.

Crop management was carried out according to the technical recommendations and technological level of the producer. In each area, three 4 × 4 m experimental plots were delineated for the LAI and f_c determinations. The observations made in the plots were used as representative of the total irrigated area (44 ha) and rainfed area (3 ha) to obtain the NDVI. The corn hybrid BG7318YH was sown on oat straw on August 8, 2018, with a population of 78,000 plants ha^{-1}; the harvest occurred on January 14, 2019. The soybean cultivar TMG 7062 was sown in succession with corn on January 24, with a population of 444,000 plants ha^{-1}; the harvest occurred on May 17, 2019. Both crops were sown with a row spacing of 0.45 m.

Observations of the LAI and the main phenological stages were carried out at intervals of approximately 8 days on two previously demarcated plants in each experimental plot. Corn leaf area was determined nondestructively by measuring the greatest width and length of fully developed leaves and estimating the area of each individual leaf via the methodology of Stickler, Wearden, and Pauli (1961). In soybean, the maximum width and length of the central leaflet of the trifoliate were measured, and the areas of the trifoliate and the plant were adjusted according to the methodology described by Richter *et al.* (2014). The LAI was determined by the ratio of the leaf area of the plant (cm^2) to the surface area occupied by that plant (cm^2).

The f_c was determined from photographs taken from the center of each plot via a Sony W800 20.1 MP circular lens digital camera with a 29 MB optical zoom (Sony Brasil, Inc.). The camera was installed on a tripod 1.20 m above the canopy and tilted 70° from the horizontal to achieve maximum visualization within the plot and minimize external influences. The field of view was 1.00 m wide and 1.20 m long, covering two rows of seeds. A 0.20 m mark was added to the ground between the crop rows to determine the scale. The image size was 576 × 1152 pixels in JPEG (*Joint Photographic Experts Group*) file format, with each image being 132 Kb. The images were recorded between 2:00 pm and 4:00 pm to avoid influences from the shadow of the crop canopy.

Once recorded, the photos were transferred to a computer for individual analysis *via* ImageJ® software (developed by *the National Institute of Health*, USA). The *software* has a selection option to set hue and saturation. Hue settings from 25--130, combined with saturation values from 10--75, correspond to green leaves (XIONG *et al*., 2019). Thus, on the basis of the scale placed on each image, the total area of the image and the area corresponding to the crop canopy and soil surface were calculated. Dividing the area corresponding to the crop canopy by the total area of the image, f_c was determined.

4.2 Irrigation management

Irrigation management was carried out by the Irriga® System, an irrigation management and monitoring service that uses a soil water depletion factor of 0.40, meaning that irrigation is recommended whenever the soil water availability falls below 40% of the total available water (TAW). The system considers the root system depth in increasing order, ranging from 0 to 0.70 m, with 0 on the day of sowing and 0.70 when the crop reaches maximum growth. Crop evapotranspiration (ETc) was calculated from the reference evapotranspiration ($_{ETo}$) and the simple crop coefficient ($Kc_{)}$, adjusted for the cropping system, crop, and soil, as proposed by Allen et al. (1998). The total irrigated depth during the cycle was 119 and 44 mm for corn and soybean, respectively.

4.3 Satellite imagery and the NDVI

The f_c and LAI for soybeans and corn were estimated via the NDVI derived from satellite imagery. The spatial imagery was obtained by the Sentinel satellite (sensors 2A and 2B). Both sensors were used in a complementary fashion, with visits staggered to cover the highest possible temporal frequency and avoid cloud cover.

To calculate the NDVI, the red and near-infrared bands, bands 4 and 8, respectively, were used. These bands have 665 nm and 842 nm band centers for the red and near-infrared, respectively, with thicknesses of 20 nm for the red band and 115 nm for the near-infrared. The spatial resolution was 10 m, and the revisit frequency of each satellite was 10 days, with the combined constellation (2A and 2B) being 5 days (EUROPE SPACE AGENCY, 2015).

The NDVI was processed via the *open-source* Google *Earth Engine library* (GORELICK *et al*., 2017) (https://earthengine.google.com/). All images with some cloud cover were discarded. The average NDVI of the total irrigated area (44 ha) and 3 ha of rainfed area was used.

4.4 Estimation of $f_{c\ NDVI}$ and IAF_{NDVI}

From the NDVI values derived from the satellite images, f_c and IAF were estimated, here called $f_{c\ NDVI}$ and IAF_{NDVI}. To estimate the $_{NDVI}$, the methodology proposed by Pôças was adopted. (2015), described in Equation (1).

$$f_{c\ NDVI} = \beta_1 \left(\frac{NDVI_i - NDVI_{min}}{NDVI_{max} - NDVI_{min}} \right) + \beta_2 \quad (1)$$

Where β_1 is an empirical coefficient (0 to 1), which depends on the maximum NDVI value at each crop development stage; ND VI $_i$ corresponds to the NDVI for a specific date; NDVI max and NDVI min are the NDVIs for the maximum and minimum vegetation cover, respectively; and β_2 corresponds to an adjustment coefficient associated with crop senescence and leaf yellowing.

The NDVI is sensitive to leaf senescence, resulting in lower values at the end of the crop cycle. Thus, β_2 it compensates for the decrease in the vegetation index due to senescence, which depends on f $_c$ (PÔÇAS *et al*., 2015). The parameters of Equation (1) were calibrated with the dataset from irrigated areas and validated with those from rainfed areas for corn and soybeans. In the calibration of the NDVImax, NDVImin, and coefficients, for β_1 and β_2, a trial-and-error procedure was used to minimize deviations between the observed and estimated values. The irrigated areas were used for calibration, and the rainfed areas were used for validation, as the rainfed areas yielded the best statistical indices.

To estimate the LAI $_{NDVI,}$ a linear regression was calibrated by relating the observed leaf area index (LAI) data to the NDVI values of the irrigated crops. This regression was subsequently validated via the LAI NDVI estimate for the rainfed areas, which was compared with the LAI estimates of the rainfed crops.

4.5 Statistical indicators

A set of statistical indicators was used to calibrate and validate the estimates of the f $_{c\ NDVI}$ and IAF $_{NDVI}$, and the estimated data were compared with the observed data (f_c obs and IAF obs). The indicators included the linear regression coefficient (b_0), coefficient of determination (R^2), root mean square error (RMSE) and percentage bias (P *bias*). b $_0$ was obtained through linear regression forced to the origin and was used to verify the under- or overestimation of the data by the model. The R^2 indicates the degree of linearity between the observed and estimated data, whereas the RMSE is the error itself, which aims for a value closer to zero (MORIASI *et al*., 2007). The P *bias* measures whether the average trend of the simulated data is greater or less than the observed values, that is, the ratio between the sum of the difference between the observed and predicted data (O $_i$ and P $_i$) and the sum of the observations (O $_i$). The ideal value of P-bias is 0; that is, low magnitude values indicate that the model simulation was accurate, while positive values indicate a tendency to overestimate the model, and negative values indicate a tendency to underestimate the model (MORIASI *et al*., 2007).

5 RESULTS AND DISCUSSION

Tables 1 and 2 present the observed values of IAF, f $_c$ and phenological stages on the date of observation for corn and soybean under irrigated and rainfed conditions.

Table 1. Dates of observations of the leaf area index (LAI), cover fraction (f_c) and phenological stages of irrigated and rainfed corn in the 2018/19 agricultural year.

Dates	Irrigated			Dryland		
	IAF	f_c	Stadium[2]	IAF	f_c	Stadiums[2]
05/09/2018	0.02	0.03	V2	0.02	0.04	V2
12/09/2018	0.02	0.05	V3	0.05	0.05	V4
September 19, 2018	0.09	0.12	V4	0.10	0.12	V4
September 26, 2018	0.32	0.21	V6	0.26	0.21	V6
10/03/2018	1.34	0.51	V8	1.15	0.46	V7
10/10/2018	1.74	0.65	V9	1.36	0.64	V8
October 18, 2018	3.26	0.75	V10	3.31	0.74	V9
October 30, 2018	5.46	0.91	V15	4.87	0.91	V13
11/13/2018	6.09	1.00	R1	6.00	1.00	V17
11/21/2018	6.08	1.00	R2	5.97	0.99	R1
11/28/2018	6.04	0.97	R3	5.88	0.96	R2
12/04/2018	6.00	0.95	R4	5.83	0.92	R4
10/12/2018	5.98	0.93	R4	5.76	0.89	R4
03/01/2019	3.17	0.84	R6	2.96	0.76	R6

[2] V represents the vegetative stage, where each number characterizes a leaf, Vt represents flowering, and R represents the reproductive stage, according to Ritchie *et al*. (1993).

Table 2. Dates of observations of the leaf area index (LAI), cover fraction (fc) and phenological stages of irrigated and rainfed soybeans in the 2018/19 agricultural year.

Dates	Irrigated			Dryland		
	IAF	f_c	Stadium [1]	IAF	f_c	Stadium [1]
February 12, 2019	1.62	0.10	V3	1.49	0.12	V4
February 19, 2019	2.57	0.17	V5	2.36	0.15	V5
February 28, 2019	3.79	0.33	V8	3.48	0.46	V8
03/04/2019	4.33	0.45	V10	3.98	0.57	V9
March 13, 2019	5.55	0.84	R1	5.10	0.82	R1
March 23, 2019	5.99	0.98	R3	5.60	0.97	R3
March 27, 2019	6.17	1.00	R3	5.80	1.00	R3
03/04/2019	6.27	1.00	R4	5.41	1.00	R4
10/04/2019	6.36	1.00	R4	5.02	1.00	R4

[1] V represents the vegetative stage, where V3 corresponds to the third node on the main stem, after the cotyledonary node, with a fully developed trifoliate, and R represents the reproductive stage, where R1 corresponds to an open flower at any node on the main stem, according to Fehr and Caviness (1977).

Figure 2 shows the temporal variation in the NDVI for the different development stages of corn and soybeans, irrigated and dryland. The NDVI increased rapidly in corn, starting 30 days after sowing, reaching a peak at the flowering stage in mid-November, and remaining above 0.6 until the end of the reproductive stage. No differences in the NDVI values were observed between irrigated and dryland corn, which can be explained by the absence of stress, since IVs do not detect mild stresses according to Pôças. *et al* . (2015). For soybean, the initial NDVI was greater than that of corn, as it is a late-season crop that is subjected to higher daily temperatures, which increases the rapid development of leaf area and height. An exponential increase in the NDVI was observed for irrigated and rainfed soybeans from the middle of the growing season onward due to the significant increase in the LAI and plant height. The NDVI plateau was observed during the reproductive period. The lack of field observations of the LAI and f_c during the physiological maturity and senescence phases is due to adverse weather conditions (rain and cloudy days), which also prevent the acquisition of the NDVI during these phases of the cycle.

Figure 2. Temporal variation in the normalized difference vegetation index (NDVI) by development stage from Sentinel images for irrigated and rainfed corn and soybean crops in the 2018/19 agricultural year, where the MF is equivalent to physiological maturity.

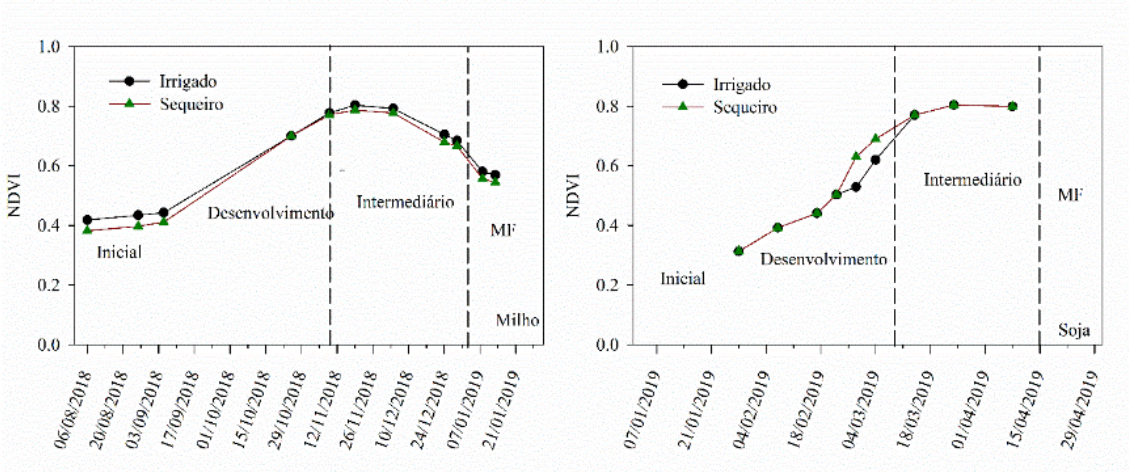

The calibrated and validated parameters of Equation 1 for irrigated and rainfed corn and soybeans are presented in Table 3. The data for the calibration of these parameters were taken from Tables 1 and 2.

Table 3. Calibrated parameters for estimating the cover fraction (f_c) via the normalized difference vegetation index (NDVI) for the 2018/2019 agricultural year.

Parameters	Crops	
	Soy	**Corn**
$NDVI_{max}$	0.75	0.75
$NDVI_{min}$	0.10	0.30
β_2	0.00	0.20
$\beta_{1\,ini}$	0.10 - 0.20	0.00 - 0.10
$\beta_{1\,dev}$	0.30 - 0.60	-
$\beta_{1\,mid}$	0.80 - 1.00	1.00
$\beta_{1\,end}$	-	1.00

$\beta_{1\,ini}$, $\beta_{1\,dev}$, $\beta_{1\,mid}$, and $\beta_{1\,end}$ correspond to the initial, development, intermediate, and final stages, respectively, as presented in Figure 2 and adapted from Pôças *et al*. (2015). (-) indicates the absence of a parameter for this variable. A value of β_2 equal to zero corresponds to a date close to physiological maturity, whereas values close to 0.5 correspond to dates close to harvest.

Calibrated NDVI values of 0.75 were observed for both crops, and NDVI values of 0.10 and 0.30 were observed for soybean and corn, respectively. The NDVI value of $_{0.10}$ coincides with the maximum canopy coverage, which occurs at the full flowering stage for both crops. The higher NDVI value of 0.30 in corn was due to the presence of still-green oats, which were desiccated close to the area where corn was planted, contributing to a higher NDVI. On the other hand, soybean was grown after corn, which had dry crop residues, not contributing to the NDVI.

For β_2, values of 0 were observed for soybeans and 0.20 for corn. The value of 0 for soybeans occurred because, on the date of the last image (04/08/2019) (Figure 2), the crop was in full development (stages V17/R4, from Table 1), and no beginning of senescence was observed, that is, the peak of the NDVI. According to Pôças *et al*. (2015), the value of β_2 compensates for the decrease in the vegetation index due to leaf senescence and yellowing, which are factors that are independent of f_c. For corn, on the other hand, a decrease in the NDVI was observed at the beginning of senescence, which was compensated by the value of β_2, indicating a less drastic reduction in f_c than in the NDVI. Values of β_2 ranging from 0 to 0.5 were reported for corn, barley, and olive crops (PÔÇAS *et al*., 2015). The values of β_1 increased linearly, ranging from 0.1 to 0.2, 0.3 to 0.6, and 0.8 to 1.0 for $\beta_{1\,ini}$, $\beta_{1\,dev}$, and $\beta_{1\,mid}$, respectively (soybean), and from 0.0 to 0.1 for $\beta_{1\,ini}$, and 1 and $\beta_{1\,mid}$ and $\beta_{1\,end}$ (corn).

The relationship between the observed coverage fraction ($f_{c\,obs}$) and the coverage fraction estimated by the NDVI ($f_{c\,NDVI}$) for corn and soybean is presented in Figure 3. A high fit between the observed and simulated values was observed for both the irrigated area (calibration) and the rainfed area (validation), with $b_{0\,values}$ close to 1.00, $R^2 > 0.99$ and P- *biases* ranging from -1.89 (irrigated) to 1.87 (rainfed) for both crops. Pôças *et al*. (2015) reported $b_{0\,values}$ of 1.07 and 1.04 and R^2 values of 0.81 and 0.96 for corn and barley, respectively. In the same study, the authors reported RMSE values of 0.10 for corn and 0.06 for barley. In the present study, RMSE values of 0.02 were observed for soybean, ranging from 0.02 (calibration) to 0.05 (validation) for corn. Although the LAI represents the effective fraction of soil covered by the canopy, the density and characteristics of the hybrid/cultivar can result in a relatively high LAI without $_{increasing\ the\ f\,c}$. This fact makes it difficult to use a single LAI value to represent the effective f_c, since the NDVI increases with the LAI, even if f_c does not increase at the same rate.

Figure 3. Relationships between $f_{c\ NDVI}$ and f_c obs of irrigated soybeans (a - calibration), rainfed soybeans (b - validation), irrigated corn (c - calibration) and rainfed corn (d - validation) in the agricultural year of 2018/19. The statistical indicators represent the linear coefficient (b_0), coefficient of determination (R^2), percentage of bias (P bias), root mean square error (RMSE) and number of observations (n).

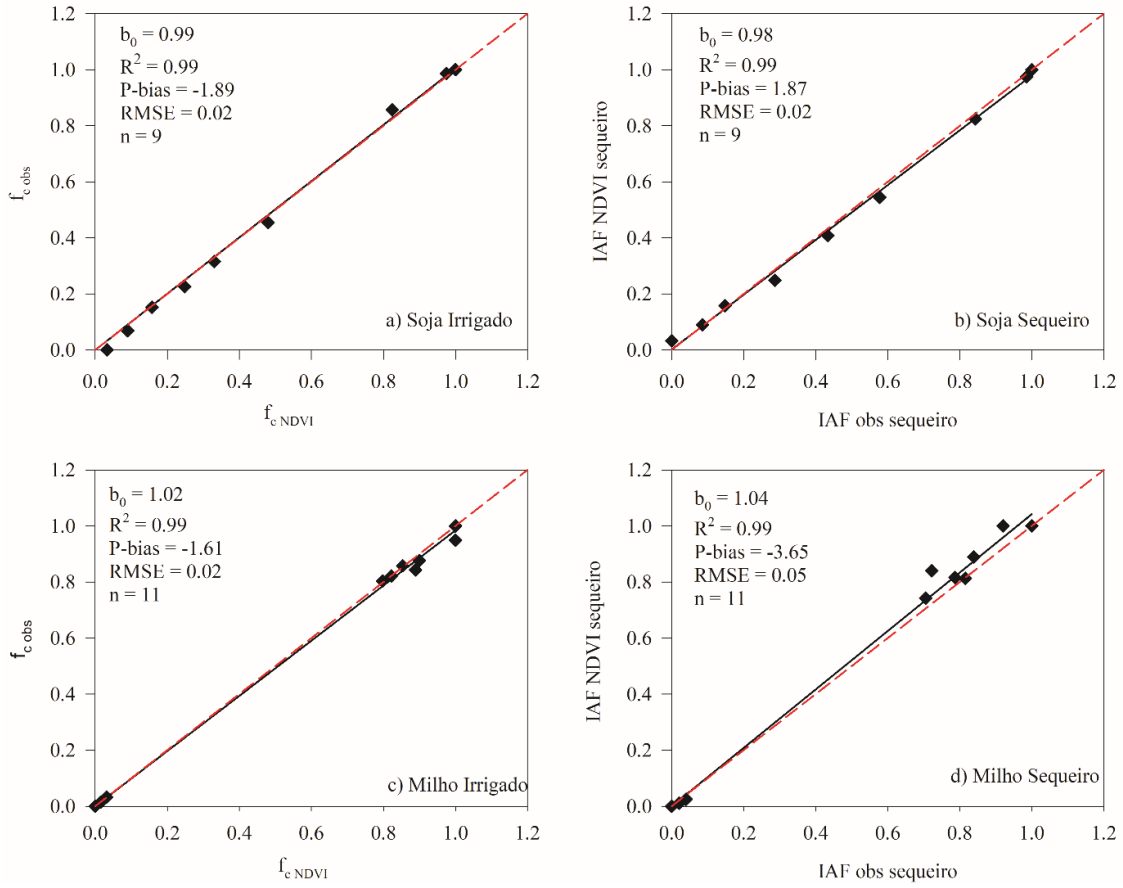

According to Campos *et al*. (2017), for many crops, including corn and soybean, the NDVI for a canopy that completely shades the soil (effective f_c) may differ from that when the LAI is at a maximum because of the relationships between the LAI and the canopy architecture and density. Consequently, f_c better represents the green soil cover by vegetation, which was also observed in this study through the linear relationship established between f c and the NDVI (Figure 3). Many authors suggest the use of f_c as a better indicator of the current state of a crop and, consequently, its transpiration, which is fundamental input data in water balance models (ROLIM *et al*., 2019). The results demonstrate that the NDVI can be widely used to monitor crop phenological stages, solar radiation interception, and water requirements, as also observed by González-Gomes *et al*. (2018).

De La Casa *et al* . (2018), using the NDVI derived from Landsat 7 and 8 satellite images with a spatial resolution of 30 m, reported a high fit between the fc estimated from photographs and that from the NDVI, with an R^2 of 0.95 for soybean. Johnson and Trout (2012) reported strong linearity between the NDVI and fc for a range of vegetable crops, such as wheat, barley, and grapevine, when they applied a general equation (f_c = 1.26 NDVI - 0.18) generated from the monitoring of 18 different species (including row crops, orchards, and grapevines) with

different maturity dates. These results are very similar to those found in this study, especially for the stages at which the canopy begins to fully cover the soil (effective fc), with a slight underestimation in the initial phase (from sowing to $_{10\%}$ LAI) due to the negative intercept.

Trout *et al* . (2008), who studied the relationship between the NDVI derived from satellite images (Landsat 5) and the f_c of several horticultural crops in commercial areas with different planting configurations and maturity stages, reported high correlations between the NDVI and the observed f_c (R^2 = 0.95) and between the observed f_c and that estimated via the NDVI (R^2=0.93), with an estimated error of 15%.

Figure 4 presents the calibration and validation of the regression models for estimating the LAI for soybean and corn. The statistical indicators used in the regression validation in Figures 3b and 3d demonstrated accuracy for estimating the LAI in rainfed areas (validation), with R^2 values ranging from 0.97 to 0.98 for soybean and corn, respectively. The b_0 values were 1.12 and 1.01, and the P biases were -14.61 and -4.08 for soybean and corn, respectively, indicating slight overestimation by the model compared with the observed data, which was greater for soybean (b_0 = 1.12).

Figure 4. Calibration and validation of linear regression to estimate the leaf area index from the normalized difference vegetation index (NDVI) derived from satellite images, using observed data from irrigated (a - calibration) and rainfed (b - validation) soybean and irrigated (c - calibration) and rainfed (d - validation) corn in the 2018/19 agricultural year. The statistical indicators presented are the linear coefficient (b $_0$), the coefficient of determination (R ^{2}), the percentage of bias (P-bias), the root mean square error (RMSE) and the number of observations (n).

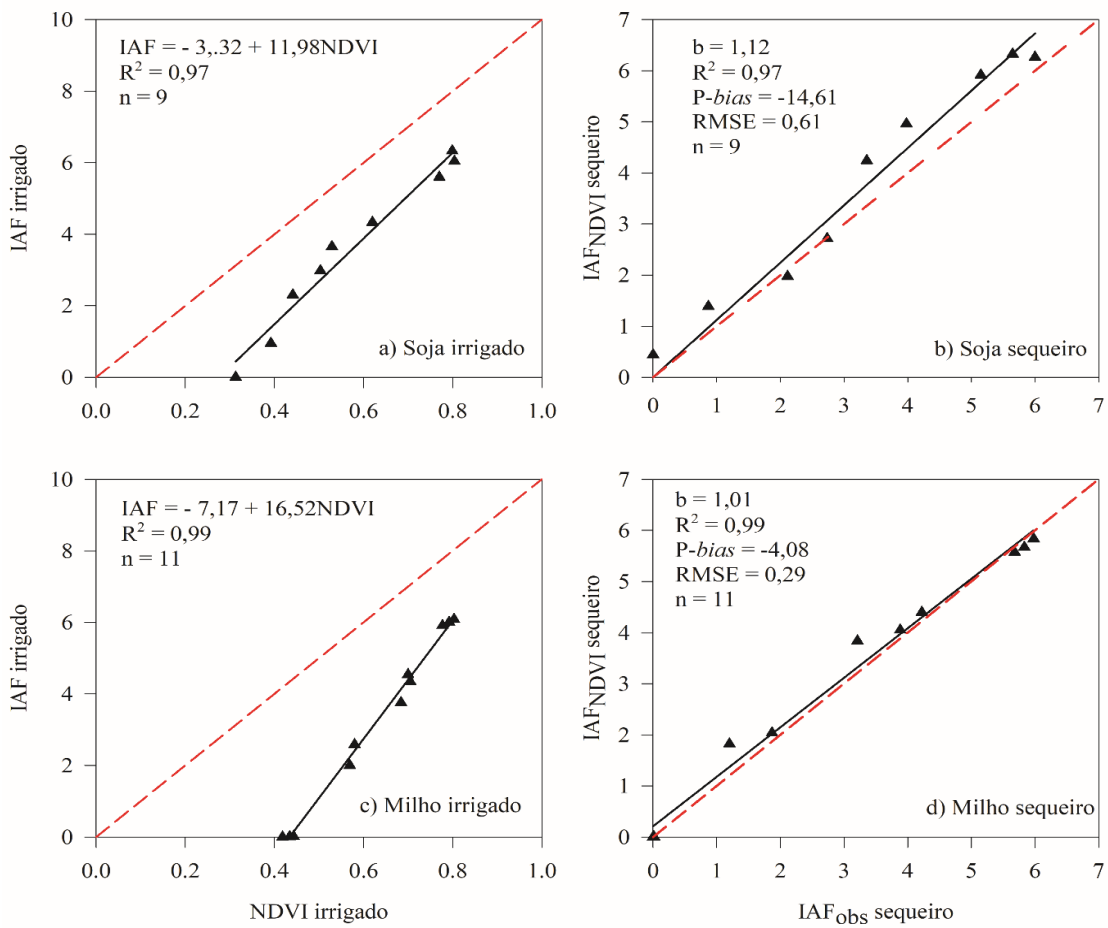

The RMSE values (0.61 and 0.29) represent 10% and 5% of the maximum LAIs found for soybean and corn, respectively, and are within the range of values reported in the literature. Zhang *et al. (2019), using* Sentinel satellite images to estimate the LAI through regressions with the NDVI, reported RMSE values between 0.44 and 0.31 for corn, which were compared with values observed at the surface. Kross *et al*. (2015), using the NDVI derived from the RapidEye satellite, with a spatial resolution of 5 m, reported mean absolute error (MAE) values of 0.64 for corn and 0.65 for soybeans, comparing the observed LAI and the LAI estimated via regressions.

The goodness of fit of the statistical indicators used to estimate the LAI $_{NDVI}$ via the equations presented, can be attributed, in large part, to the use of satellite images with high spatial resolution (10 m), as is the case with sensors 2A and 2B onboard the Sentinel satellite. However, even when the NDVI is derived via images with a spatial resolution of 250 m (MODIS), Richetti *et al*. (2019) concluded that the LAI derived from the NDVI presented similar results to the LAI observed in the field for the calibration of CSM-CROPGRO-Soybean.

6 C ONCLUSION

The f_c estimated from the NDVI showed a linear relationship, with a good fit, on the basis of the calibration of the parameters of the equation proposed by Pôças *et al*. (2015), with RMSEs of 0.02 and 0.05, for soybean and corn, respectively, in validating the model parameters. The regressions proposed for estimating the LAIs of both crops are also effective, with RMSEs of 0.61 and 0.29 for soybean and corn, respectively. Thus, the proposed models were efficient for monitoring the biophysical variables f_c and LAI.

7 ACKNOWLEDGMENTS

The authors would like to thank the Coordination for the Improvement of Higher Education Personnel (CAPES) for granting a master's scholarship to the first author.

8 REFERENCES

ALLEN, RG; PEREIRA, LS Estimating crop coefficients from fraction of ground cover and height. **Irrigation Science** , Berlin, v. 28, no. 01, p. 17-34, 2009. DOI: 10.1007/s00271-009-0182-z. Available at: https://link.springer.com/article/10.1007/s00271-009-0182-z. Accessed on: 8 June. 2020.

ALLEN, RG; PEREIRA, LS; RAES, D.; SMITH, M. **Crop evapotranspiration** - Guidelines for computing crop water requirements. Rome: FAO, 1998. 300 p. (Irrigation and Drainage Paper , 56). Available at: https://www.fao.org/3/x0490e/x0490e00.htm . Access on : June 12, 2020.

ASADI, S.; BANNAYAN, M.; JAHAN, M.; HISSEINI, AF Using the red-near infrared spectra to estimate ground cover based on vegetative indices . **International Journal of Remote Sensing** , Basingstoke, v. 49, n. 18, p. 7153-7168, 2019. DOI: 10.1080/01431161.2019.1601282. Available at: https://www.tandfonline.com/doi/abs/10.1080/01431161.2019.1601282?journalCode=tres20 . Access on : June 12, 2020.

BARKER, JB; NEALE, CMU; HEEREN. MD; SUYKER, AE Evaluation of a hybrid reflectance-based crop coefficient and energy balance evapotranspiration model for irrigation management. **Transaction of the ASABE** , St. Joseph, v. 61, no. 2, p. 533-548, 2018. DOI: 10.13031/trans.12311. Available at: https://elibrary.asabe.org/abstract.asp?AID=48890&t=3&dabs=Y&redir=&redirType=. Access on : June 14, 2020.

CAMPOS, I.; NEALE, CMU; ARKEBAUER, TJ; SUYKER, AE; GONÇALVES, IZ Water productivity and crop yield: A simplified remote sensing driven operational approach. **Agricultural and Forest Meteorology** , Amsterdam, v. 249, n. 1, p. 501-511, 2018. DOI: 10.1016/j.agrformet.2017.07.0187. Available at: https://www.sciencedirect.com/science/article/pii/S0168192317302344?casa_token=qsWnXEmLlbIAAAAA:um46g7ZoYHWdqJDj-jc8AppZG-sCCoS7TwSzBh . Accessed on: June 13, 2020.

CAMPOS, I.; NEALE CMU; ARKEBAUER, T.J.; SUYKER, AE; GONÇALVES, IZ Reflectance-based crop coefficients REDUX: For operational evapotranspiration estimates in the age of high producing hybrid varieties. **Agricultural Water Management** , Amsterdam, v. 187, p. 140-153, 2017. DOI: 10.1016/j.agwat.2017.03.022. Available at: https://www.sciencedirect.com/science/article/pii/S0378377417301026 . Accessed on: June 13, 2020.

DE LA CASA, A.; OVANDO, G.; BRESSANINI, L.; MARTÍNEZ, J.; DÍAZ, G.; MIRANDA, C. **ISPRS Journal of Photogrammetry and Remote Sensing** , Amsterdam v. 146, p. 531-547, Soybean crop coverage estimation from NDVI images with different spatial resolution to evaluate yield variability in a plot.2018. DOI: 10.1016/j.isprsjprs.2018.10.018. Available at: https://www.sciencedirect.com/science/article/pii/S092427161830296X . Access on : June 4, 2020.

FEHR; WR; CAVINESS, C.E. **Stages of soybean development** . Ames: Cooperative Extension Service , 1977. (Special Bulletin, 80). Available at: https://dr.lib.iastate.edu/entities/publication/58c89bfe-844d-42b6-8b6c-2c6082595ba3 . Access on : June 2, 2020.

FOSTER, T.; BROZOVIĆ, N.; BUTLER, A.P.; NEALE, C.M.U.; RAES, D.; STEDUTO, P.; FERERES, E.; HSIAO, T.C. AquaCrop -OS: An open source version of FAO's crop water productivity model. **Agricultural Water Management** , Amsterdam, v. 181, p. 18-22, 2017. DOI: 10.1016/j.agwat.2016.11.015. Available at : tps://www.sciencedirect.com/science/article/pii/S0378377416304589#:~:text=In%20this%20study%2C%20we%20present, programming%20languages%20and%20operating%20systems. Access on : June 18, 2020.

GAO, F.; ANDERSON, M.; DAUGHTRY, C.; JOHNSON, D. Assessing the Variability of Corn and Soybean Yields in Central Iowa Using High Spatiotemporal Resolution Multi-Satellite Imagery. **Remote Sensing ,** Basel v. 10, n. 1489, p. 1-22, 2018. DOI: 10.3390/rs10091489. Available at: https://www.mdpi.com/2072-4292/10/9/1489 . Access on : June 18, 2020.

GONZÁLEZ-GÓMEZ, L.; CAMPOS, I.; CALERA, A. Use of different temporal scales to monitor phenology and its relationship with temporal evolution of normalized difference vegetation index in wheat. **Journal of Applied Remote Sensing** , Bellingham, vol. 12, no. 2, p. 1-10, 2018. DOI : 10 . 1117/1.jrs.12.026010. Available at: https://www.spiedigitallibrary.org/journals/journal-of-applied-remote-sensing/volume-12/issue-2/026010/Use-of-different-temporal-scales-to-monitor-phenology-and-its/10.1117/1.JRS.12.026010.short?SSO=1 . Access on : June 18, 2020.

GORELICK, N.; HANCHER, M.; DIXON, M.; ILYUSHCHENKO, S.; THAU, D.; MOORE, R. Google Earth Engine: Planetary-scale geospatial analysis for everyone. **Remote Sensing of Environment** , Amsterdam, v. 202, p. 18-27, 2017. DOI: 10.1016/j.rse.2017.06.031. Available at: https://www.sciencedirect.com/science/article/pii/S0034425717302900 . Access on : June 19, 2020.

JOHNSON, L. F.; TROUT, TJ Satellite NDVI assisted monitoring of vegetable crop evapotranspiration in California's San Joaquin valley. **Remote Sensing ,** Basel, v. 4, n. 2, p. 439-455, 2012. DOI: 10.3390/rs4020439. Available at: https://www.mdpi.com/2072-4292/4/2/439 . Access in : June 16, 2020.

KROSS, A.; MCNAIRN, H.; LAPEN, D.; SUNOHARA, M.; CHAMPAGNE, C. Assessment of RapidEye vegetation indices for estimation of leaf area index and biomass in corn and soybean crops. **International Journal of Applied Earth Observation and Geoinformation** , Amsterdam, v. 34, p. 235-248, 2015. DOI: 10.1016/j.jag.2014.08.002. Available at: https://www.sciencedirect.com/science/article/pii/S0303243414001664 . Access on : June 8, 2020.

LI, Y.; CHENA, D.; WALKER, CN; ANGUS, JF Estimating the nitrogen status of crops using a digital camera. **Field Crops Research .** , Amsterdam, v. 118, n. 3, p. 221-227, 2010. DOI: 10.1016/j.fcr.2010.05.011 . Available at: https://www.sciencedirect.com/science/article/pii/S0378429010001358 . Accessed on: June 6 , 2020.

LÓPEZ-URREA, R.; SÁNCHEZ, JM; DE LA CRUZ, F.; GONZÁLEZ-PIQUERAS, J.; CHAVES, JL Evapotranspiration and crop coefficients from lysimeter measurements for sprinkler-irrigated canola . **Agricultural Water Management** , Amsterdam , v. 239 , p. 1-10, 2020. DOI 10.1016/j.agwat.2020.106260. Available at: https://www.sciencedirect.com/science/article/pii/S0378377420302110 . Accessed: June 20, 2020.

MORIASI, D, N.; ARNOLD, JG; VAN LIEW, MW; BINGNER, RL; HARMEL, RD; VEITH, TL Model evaluation guidelines for systematic quantification of accuracy in watershed simulations. **Transactions of the ASABE** , St. Joseph, vol . 50, no. 3, p. 885-900, 2007. DOI: 10.13031/2013.23153 . Available at https://www.researchgate.net/publication/43261199_Model_Evaluation_Guidelines_for_Systematic_Quantification_of_Accuracy_in_Watershed_Simulations . Access on : June 12, 2020.

NEALE, CMU; GELI, HME; KUSTAS, W.P.; ALFIERI, JG; GOWDA, PH; EVETT, SR; PRUEGER, JH; HIPPS, LE; DULANEY, W.P.; CHAVEZ, JL; FRENCH, AN; HOWELL, TA Soil water content estimation using a remote sensing based hybrid evapotranspiration modeling approach. **Advances in Water Resources** , Amsterdam v. 50, p. 152-161, 2012. DOI: 10.1016/j.advwatres.2012.10.008. Available at: https://www.sciencedirect.com/science/article/pii/S0309170812002709 . Access on : June 14, 2020.

PAREDES, P.; RODRIGUES, G.; PETRY, M.; SEVERO, P.; CARLESSO, R.; PEREIRA, LS Evapotranspiration Partition and Crop Coefficients of Tifton 85 Bermudagrass as Affected by the Frequency of Cuttings. Application of the FAO56 Dual Kc Model. **water** , Basel v. 10, n. 5 p. 558-578, 2018. DOI: 10.3390/w10050558. Available at: https://www.mdpi.com/2073-4441/10/5/558 . Accessed on: June 14, 2020.

PAREDES, P.; RODRIGUES, GC; CAMEIRA, MR; TORRES, MO; PEREIRA LS Assessing yield, water productivity and farm economic returns of malt barley as influenced by

the sowing dates and supplemental irrigation. **Agricultural Water Management** , Amsterdam , v. 179, n. 1, p . 132-143, 2017. DOI: 10.1016/j.agwat.2016.05.033. Available at: https://www.sciencedirect.com/science/article/pii/S0378377416302013 . Access in : June 4, 2020.

PÔÇAS, I.; CALERA, A.; CAMPOS, I.; CUNHA, M. Remote sensing for estimating and mapping single and basal crop coe ffi cients : A review on spectral vegetation indices approaches. **Agricultural Water Management** , Amsterdam , vol. 233, p. 106081, 2020. DOI: 10.1016/j.agwat.2020.106081 . Available at: https://www.sciencedirect.com/science/article/pii/S0378377419322498 . Accessed on: June 2, 2020.

PÔÇAS, I.; PAÇO, T.; PAREDES, P.; CUNHA, M.; PEREIRA, LS Estimation of actual crop coefficients using remotely sensed vegetation indices and soil water balance modeled data. **Remote Sensing** , Basel , v. 7, p. 2373-2400 , 2015 . DOI: 10.3390/rs70302373. Available at: https://www.mdpi.com/2072-4292/7/3/2373 . Access on : June 2, 2020.

PURCELL, L. C.; BALL, RA; REAPER, JD; VORIES, ED Radiation use efficiency and biomass production in soybean at different plant population densities. **Crop Science** , Madison , vol. 42, no. 1, p. 172-177, 2002. DOI: 10.2135/cropsci2002.1720. Available at: https://acsess.onlinelibrary.wiley.com/doi/abs/10.2135/cropsci2002.1720 . Access on : June 20, 2020.

RICHETTI, J.; BOOTE, KJ; HOOGENBOOM, G.; JUDGE, JA; URIBE-OPAZO, MA Remotely sensed vegetation index and LAI for parameter determination of the CSM-CROPGRO-Soybean model when in situ data are not available. **International Journal of Applied Earth Observation and Geoinformation** , Amsterdam, v. 79, n. 1, p . 110-115, 2019. DOI: 10.1016/j.jag.2019.03.007 . Available at: https://www.sciencedirect.com/science/article/pii/S0303243418307372?via%3Dihub . Accessed on: June 18, 2020.

RICHTER, GL; ZANON, AJ; STRECK, NA; GUEDES, JVC; KRÄULICH, B.; ROCHA, TSM; WINCK, JEM; CERA, JC Estimation of leaf area of old and modern soybean cultivars by nondestructive method. **Bragantia ,** Campinas , v. 73, n. 4, p. 416-425, 2014. DOI : 10.1590/1678-4499.0179. Available at: https://www.scielo.br/j/brag/a/5t8dfDshhDZFcwQq4rZZ8Cz/abstract/?lang=pt . Access on : June 19, 2020.

RITCHIE, SW; HANWAY, JJ; BENSON, GO **How a corn plant develops** . Ames: Iowa State University, 1993. (Special Bulletin, n. 48). Available at : https://http://publications.iowa.gov/18027/1/How%20a%20corn%20plant%20develops001.pdf . Access on : June 11, 2020.

RITCHIE, GL; SULLIVAN, DG; VENCILL, W.K.; BEDNARZ, CW; HOOK, JE Sensitivities of normalized difference vegetation index and a green/red ratio index to cotton ground cover fraction. **crop science** , Madison, v. 50, n. 3, p. 1000-1010, 2010. DOI: 10.2135/cropsci2009.04.0203 . Available at: https://acsess.onlinelibrary.wiley.com/doi/abs/10.2135/cropsci2009.04.0203 . Accessed on: June 9, 2020.

ROLIM, J.; NAVARRO, A.; VILAR, P.; SARAIVA, C.; CATALÃO, J. Crop retrieval using Earth observations data to support agricultural water management. **Agricultural Engineering** , Jaboticabal, v. 39, n. 3, p. 380-390, 2019. DOI: 10.1590/1809-4430-Eng.Agric.v39n3p380-390/2019 . Available at: https://www.scielo.br/j/eagri/a/MKtwmL5fG58yTK3VGS5DMyd/?format=html&lang=en . Access on : June 7, 2020.

SAKAMOTO, T.; WARDLOW, BD; GITELSON, AA; VERMA, SB; SUYKER, AE; ARKEBAUER, TA Two-Step Filtering approach for detecting maize and soybean phenology with time-series MODIS data. **Remote Sensing of Environment,** Amsterdam, v. 114, n. 10, p. 2146-2159, 2010. DOI: 10.1016/j.rse.2010.04.019. Available at: https://www.sciencedirect.com/science/article/pii/S003442571000132X . Access on : June 5, 2020.

STICKLER, FC; WEARDEN, S.; PAULI, AW Leaf Area Determination in Grain Sorghum. **Agronomy Journal** , Madison, v. 53, n. 3, p. 187-188, 1961. DOI: 10.2134/agronj1961.00021962005300030. Available at: https://acsess.onlinelibrary.wiley.com/doi/abs/10.2134/agronj1961.00021962005300030018x . Access on : June 3, 2020.

TROUT, T.J.; JOHNSON, L. F.; GARTUNG, J. Remote Sensing of Canopy Cover in Horticultural Crops. **HortScience** , Alexandria, v. 43, no. 2, p. 333-337, 2008. DOI: 10.21273/HORTSCI.43.2.333 . Available at: https://journals.ashs.org/hortsci/view/journals/hortsci/43/2/article-p333.xml#:~:text=Canopy%20cover%20(CC)%20is%20an,water%20use%20in%20horticultural%20crops.&text=These%20results%20indicate%20that%20remotely,water%20demand%2C%20of%20horticultural%20crops . Access on : June 1, 2020.

XIONG, Y.; WEST, CP; BROWN, CP; GREEN, PE Digital Image Analysis of Old World Bluestem Cover to Estimate Canopy Development. **Agronomy Journal** , Madison, v . 3, n. 3, p. 1247-1253, 2019. DOI: 10.2134/agronj2018.08.0502 . Available at: https://hdl.handle.net/2346/86941 . Access on . June 3, 2020.

YAO, F.; TANG, P.; WANG, P.; ZHANG, J. Estimation of maize yield by using a process-based model and remote sensing data in the Northeast China Plain. **Physics and Chemistry of the Earth** , Amsterdam , vol. 87, no. 88 p. 142-152, 2015. DOI: 10.1016/j.pce.2015.08.010. Available at: https://www.sciencedirect.com/science/article/pii/S1474706515000960 . Access on : June 1, 2020.

ZHANG, M.; SU, W.; FU, Y.; Zhu, D.; XUE, JH; HUANG, J.; WEI, W.; Wu, J.; YAO, C. Superresolution enhancement of Sentinel-2 image for retrieving LAI and chlorophyll content of summer corn. **European Journal of Agronomy,** v. 111, n. 11, p. 125-137, 2019. DOI: 10.1016/j.eja.2019.125938 . Available at: https://www.sciencedirect.com/science/article/pii/S1161030119300759?casa_token=OGndc-GDHD4AAAAA:I3BgI-

MZwxqsMmjOo8anyyh7NB3yDxcQjwjeFQIlpCVz_YVz26kiEiiUerdGY97IpzdTcG0ZEaFq
. Access on : June 17, 2020.